Evaluation of Exponential Factor on Boundary Value Problem of Inverse Distance Weighting Method of Interpolation.

Pius Onoja IBRAHIM, Nigeria, Harald STERNBERG, Germany

Key words: Inverse distance weighting **(**IDW), Boundaries, Discrete data, Reservoir, Bathymetry

SUMMARY

Bathymetric information about waterbody is of great importance to many professionals for the installation of moles, ducts, marinas, bridges, tunnels, mineral prospecting, waterways, dredging, silting control of the river, building or reassessing port dimensions, and lakes among others. Depths information about the presence of such a submerge area on a map is obtained via a bathymetric survey. But acquiring this information is economically cost implicative. Managers are deriving ways of getting adequate information about seafloor from using the conventional lead line to an advanced method of imploying single beam echosounder. Information is lost because of the single footprint of this instrument. Another challenge is that it is time consuming depending on the area of study. Since this instrument is limited in coverage, researchers have devised means of obtaining sparse information and then use interpolation to densify the data. Inverse distance weighting (IDW) has been employed to interpolate sounding data with discrepancies at the boundaries. Consequently, this study tends to investigate the behavioural pattern of IDW based on exponential value and how it affects boundaries.

Evaluation of Exponential Factor on Boundary Value Problem of Inverse Distance Weighting Method of Interpolation.

Pius Onoja IBRAHIM, Nigeria, Harald STERNBERG, Germany

1. INTRODUCTION

The art and scientific study of nature, physical and chemical properties of features on, in or beneath waterbody to effectively mapped out its configuration from sets of measurement (depth, shoreline, tide, etc.) is referred to as hydrography (Ingham, 1984; IHO, 2019). This aspect of waterbody investigation gave birth to a specialized area of hydrography known as bathymetry survey "the determination of variation in-depth for a detailed presentation of the waterbed topography (Marian et al., 2012; Hell et al., 2012;). The information gained aid better understanding and interpretation to enhance the activities of marine navigation, dredging, offshore oil and gas exploration drilling, marine construction and other related operations within and outside waterbody environment (Ojigi et al., 2010; Hell et al., 2012; IHO, 2018). The information measured from a bathymetric survey is used to generate a map called nautical chart from which further information about other sections can be extracted (Igham, 1984).

However, acquiring data via this method for the actual presentation of the seafloor have metamorphosed from the traditional method to the most sophisticated method with better resolution "lead line to single beam echosounder, swath beam echosounder to multibeam echosounder, and multibeam to side-scan sonar" nevertheless, each of this instrument method of data acquisition has its drawback. Most recent is the use of single beam or multibeam echosounder in connection with differential global navigation satellites system (DGNEE e.g. DGPS) to acquire spatial data "x, y, z" (Vermeyen, 2006; Hilldale and Raff, 2008). Thus, due to wider area of coverage and high cost of executing such bathymetry task, discrete data are acquired (Stefan et al., 2017) and afterwards interpolated for Digital Elevation Model (DEM) generation for spatial representation of the waterbed (Silverira, 2014; Ajayi et al., 2018). Consequently, the elevation/depths of the scanty area can be extracted (Lampe and Morlock, 2007; Hansen, 2007). Hence, the overall data can be used to compute the storage capacity of the area under study.

Furthermore, to understand the physical feature and content of the waterbody from bathymetric data, a spread of information is needed. In a situation where the information is scanty "especially from a single beam echosounder", interpolation is used to account for the sparse area (Silverira, 2014). Although, data may be incomplete in two different ways: the absence of values in a dataset or the absence of values for locations in a geographic landscape (Yongwan and Daniel, 2013), therefore prediction is necessary to account for the sparse region. Among the methods of interpolation are Kriging, Inverse distance weighting, Radial basis functions, etc. consequently, the Inverse distance weighting technique has found wide application by practitioners due its robustness and simplicity (Goff and Nordfjord, 2004; Merwade et al., 2006). However, with discrepancies at the boundaries depending on exponent power imployed.

This setback at the boundaries will yield a poor output considering determining the storage capacity of a reservoir from discrete bathymetry data interpolated via IDW. Consequently, this study tends to investigate the behavioural pattern of IDW based on exponential value and how it affects boundaries and the volumetric capacity of a reservoir.

2. INVERSE DISTANCE WEIGHTING: AN OVERVIEW

Inverse distance weighting technique of estimation is also referred to as a deterministic method of interpolation; because the model utilizes mathematical functions for estimation (Ferreira, 2015). In addition, deterministic interpolation techniques are classified into two sets; Local and Global. Their major difference is how they considered data during estimation (White and Hodges, 2005). The global deterministic takes the entire dataset into account during prediction, while the local deterministic considered dataset within its neighbourhood for densification. The decision of whether the surface should follow the pattern of the dataset or not is based on deterministic interpolator (Lark, 2009). However, there are exact and inexact predictions: if the prediction matches exactly the dataset, the interpolator is said to be an exact interpolator, and if there is a tremendous divergent between the measured value and the estimated value it is referred to as inexact interpolator (Petersen et al., 2008). This spatial prediction technique also referred to as spatial interpolation technique has received a wide application because of its simplicity, intuitiveness, and fastness to compute (Landim, 2000; Ferreira, 2015). In contrast, it also has some cons associated with it, such as choice of interpolation parameters, the interpolation is always exact "no smoothing," sensitive to outliers and sampling configuration "clustered and isolated points" (Marcelo *et al*., 2015; Italo *et al.,* 2017).

This method of special prediction techniques does not involve statistical criterion when performing the experiment, which made it globally adopted as a dependable means of estimation. Hence, when a deterministic criterion is employed, determining the dependability are randomly chosen (Borga and Vizzaccaro 1997). Over the year's researchers have been developing models to improve this interpolation technique: among which are Grid Inverse Distance Weighting as described by (Nalder and Wein 1998) "thus, the method involves using a regression process to predict the unknown from the climatic properties of the known points," Selective Inverse Distance Weighting (SIDW) (Ballarin et al., 2017) etc. Though, each of this method is used base on the purpose and type of data to be interpolated.

2.1 Evaluating Inverse distance models

This method of interpolation has been appraised by various authors (Sonza, 2003; Marcelo et al., 2015; Ferreira, 2015; and Meng and Borders, 2013) as a robust method of representing waterbed configuration (Digital Elevation Model) because of its smoothness of representing the model location, in addition, its liberty of assigning dimension parameters within neighbourhood. The fundamental assumption of inverse distance weighted interpolation is that of a positive spatial autocorrelation (Olena and Clayton, 2008); the relationship between neighbouring dataset is highly correlated than that of a distant dataset (Yang et al., 2006; Landim, 2000). This is supported by equation 1:

$$\mathrm{H}_P = \frac{\sum_{i=1}^{n}\left(\frac{H_i}{d_i^p}\right)}{\sum_{i=1}^{n}\left(\frac{1}{d_i^p}\right)} \qquad \text{equation 1.}$$

Where H is the reduced water depth, p is the exponent power employed, d is the separation bandwidth which is evenly distributed on the interpolation surface from node to node, and occasionally in default by the mechanism. However, the default can be altered by the analyst based on the intended purpose of interpolating the data. The sigma notation indicates summing the entire points needed for interpolation; however, in this case summing the H values at the region with respect to distance. There will be no effect on the interpolated surface (H_P) if the value of the denominator is small (more distance).
Furthermore, Shepard (1968) presented a prevalent form of estimating H value from a known point X depending on the samples data: $H_i = H(X_i)\ for\ \ i = 1, 2, 3 \ldots, n$ and in extension it is expressed as;

$$H_{(X)} = \begin{cases} \frac{\sum_{i=1}^{N} \omega_i(X)_{H_i}}{\sum_{i=1}^{N} \omega_i\,(X)} & \begin{pmatrix} if\ d(X, X_i) \neq 0\ for\ all\ i \\ if\ d(X, X_i) = 0\ for\ some\ i \end{pmatrix} \\ Hi & \end{cases} \qquad \text{equation 2}$$

The weight function $\omega_i(X) = \frac{1}{d(X,X_i)^p}$ equation 3

Where X is the expected interpolated point, X_i is the sample known point, d is the distance from the known point to the predicted point, N is the total sample size, while p is the power exponent and a positive real number. Also, IDW is the georeferenced weighted average of known points within a specified neighbourhood (Shepard 1968; Franke 1982; Diodato and Ceccarelli 2005) and mathematically given as:

$$(Z^{*}H) = \sum_{i=1}^{N} \lambda_i Z(H_{\boldsymbol{i}}) \qquad \text{equation 4}$$

where H is the inference region, $H_{\boldsymbol{i}}$ = 1,2,3,...,n are the known region data, while Z*(H) is the inverse distance estimator at the region, N is the total points within the neighbourhood, λ_i (i = 1,...,n) is the attributed weight to each search area, are the weights assigned to each sample point, and $Z(H_{\boldsymbol{i}})$ i = 1,2,3,...,n are the considered known points at a sub-region. The weight is calculated by

$$\lambda_i = \frac{\frac{1}{d_i{}^p}}{\sum_{i=1}^{N}\left(\frac{1}{d_i{}^p}\right)} \qquad \text{equation 5}$$

Provided that: $\sum_{i=1}^{N} \lambda_i = 1$
The parameters $(d\ and\ p)$ are separation distances and exponent. The weight is usually roundup as 1. The value of the weight is a function of distances “the higher the distance value

the lower the weight vice-visa," for a higher value of p the interpolated surface will become a plain surface of equal depth value (Diodato and Ceccarelli, 2005).

To measure the degree of accuracy and conformity of the predicted surface to the unknown data via IDW, Olena and Clayton (2008), proposed a statistical formalism by introducing an estimation variance at the unknown area to determine the degree of reliability of the output. The statistical formalism introduced are based on stationarity "a two-phase requirement for conducting statistical prediction." Firstly, that the dataset has a common mean throughout the region A, and secondly, that the variance is fixed thought the region A (Deutsch, 2002). This is expressed as:

$$\mathrm{E}\big(Z(H)\big) = m, \quad \forall H \in A \qquad \text{equation 6}$$

$$Var\big(Z(H)\big) = \mathrm{E}(Z(H) - m(H))^2 = \sigma^2, \quad \forall H \in A \qquad \text{equation 7}$$

Therefore, relating this to IDW estimator (Z^*H) to a region H and the postulated stationarity; thus, the mean and variance is given as:

$$\mathrm{E}(Z^*H) = \mathrm{E}(\textstyle\sum_{i=1}^{N} \lambda_i Z(H_i)) \qquad \text{equation 8}$$
$$= \textstyle\sum_{i=1}^{N} \lambda_i \mathrm{E}\big(Z(H_i)\big) = m \sum_{i=1}^{N} \lambda_i = m$$

$$Var(Z^*H) = Var(\textstyle\sum_{i=1}^{N} \lambda_i Z(H_i))$$
$$= \textstyle\sum_{i=1}^{N} \sum_{i=1}^{N} \lambda_i \lambda_i \, Cov\big(Z(H_i), Z\big(H_j\big)\big) \qquad \text{equation 9}$$

The $Cov\big(Z(H_i), Z\big(H_j\big)\big)$ is the data-data covariance model computed based on stationarity conditions and assume symmetric subject to semivariogram model $2\gamma(H)$ (Journel and Huijbregts 1978; Noel and Andrew 2016). These statistical estimators are determined at the data region base on the dataset value; the subregion variance and the stationarity variance σ^2 converge at a definite point providing an avenue for assessment. In the stationarity, the local variance at each section should be equal to the global variance. Another factor to consider is the smoothing effect, which minimises the degree of errors associated with this method of spatial interpolation technique. The smoothing effecting is given as:

$$Smoothing\ effect = \sigma^2 - var(Z^*H)$$
$$= \sigma^2 - \textstyle\sum_{i=1}^{N} \sum_{i=1}^{N} \lambda_i \lambda_i \, Cov\big(Z(H_i), Z\big(H_j\big)\big) \qquad \text{equation 10}$$

Furthermore, there is a correlation between Inverse distance weighting estimator and Inverse distance weighting variance, as presented in equation 10, which is also referred to as a missing variance. Summing the smoothing effect equation and IDW model a new function is obtained whose variance is equal to the stationary global variance σ^2 : therefore, to determine the global variance at a region $\boldsymbol{H}$ the statistical equation…. is used (Deutsch, 2002; Olena and Clayton, 2008).

$$\sigma_{est}^2 = \mathrm{E}[Z - Z^*(H)]^2$$

$$= \sigma^2 - 2\sum_{i=1}^{N} \lambda_i Cov(Z(H_i), Z(H)) + \sum_{i=1}^{N}\sum_{i=1}^{N} \lambda_i \lambda_i \, Cov\big(Z(H_i), Z\big(H_j\big)\big) \qquad \text{equation 11}$$

However, the introduction of minimum error variance model into IDW is to enhance its accuracy further and to accommodate continuous-discrete data (Andreas and Jukka, 2015); although, the data has to be distributed into sub-data and then processed. This approached will be tedious considering the large volume of data, and as such different output will be obtained and later merged as one entity. Consequently, errors may result in the compilation of results.

2.2 Evaluating exponent power and boundaries

The exponential power is a key component that determines the spread and elevation of the predicted data. The effectiveness of exponent value to IDW spatial interpolation is pronounced when the sample data of the study area are adequately spread, especially about a discrete object, "discrete objects are objects with definite shapes such as water bodies, roads, buildings (Andreas and Jukra, 2015)." However, the results from this method vary depending on the exponent value for instance: low exponents (0-2) stress local anomalies; high exponents (3-5) soften local anomalies; and higher or equal exponents up to 10 results in even estimates (Landim, 2000). If these arguments hold, there will be bulging at the boundaries, and calculating the cubic content of discrete objects will be erroneous at the lower exponent power, and the tendency for inequality of Z value at the boundaries even after predefined is obvious.
Since this method of spatial interpolation is sensitive to exponent value, the number of neighbouring points and their distance apart, hence, the need to precisely determine the best-fit exponent and bandwidth that adequately match the spatial data characteristic depends entirely on the analyst. In addition, several authors recommendations regarding the best-fit exponent are divergent. For instance, the following authors proposed; Morrison (1974), $3 \le k \le 7$; MacDougall (1976), $6 \le k \le 9$; Peucker (1980), $k \le 6$; and Hodgson (1992), $4 \le k \le 7$; While Declercq (1996), suggested that $4 \le k \le 8$, $16 \le k \le 24$ favours smooth and rugged surfaces respectively. Contrarily to this is presented by Landim (2000), that $0 \le k \le 2$, $3 \le k \le 5$, and $5 \le k \le 10$ results in; stress local anomalies, soften local anomalies, and equal Z estimates throughout the surfaces respectively.

3. DATA DESCRIPTION AND METHODOLOGY APPLIED

To evaluate the effectiveness of IDW spatial interpolation technique over a discrete object such as a reservoir. This interpolation method was employed to interpolate Tagwai Dam bathymetric data. The sounding data was explicitly acquired for research purposes by the Authors. The total area of the reservoir at the instant of surveyed is 3,020,344.936m^2 (302.035hect) with a perimeter of 8,728.358m. The maximum depth observed was 21.400m. The reduced water level at the moment of sounding was 250.170m, which was referenced to a sounding datum established around the corridor of the reservoir. The bathymetric dataset was reduced to the water level, and the maximum and minimum data was 250.170m and 228.770m, respectively. The total spatial points data was 673, including 90 shorelines delineated points data, which was observed by traversing the entire reservoir to define the discrete object adequately. With a total of 17 cross sectional strips. Figure 1 describes the strip pattern of the sample data; in addition, is the defined shoreline information to enhance the estimation process of the discrete object spatially.

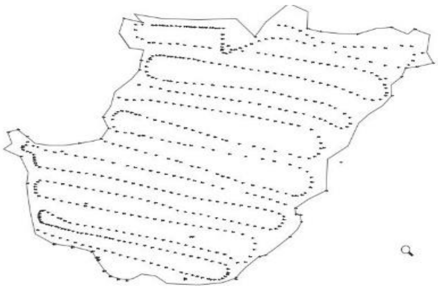

Figure 1: Sample data-Tagwai Reservoir in Nigeria (Sour: Research lab)

The experiment was conducted in the interface of IDW spatial interpolation techniques with optimal parameters chosen to achieve effective output. The spatial spacing was set at 27.323m, 27.200m in the X and Y directions respectively, with a linear Z transformation. The search geometric ellipse radius was projected at 1550m and 1550m in both axes, while the anisotropy ratio and angle were left at the default of 1 and 0. The number of neighbouring sample data determine the accuracy of the estimated location, in view of this: the following parameters were used to enhance the experimental results; the number of sectors to search was 4, maximum data to use from all sectors was 64, maximum data from each sector was 16, minimum data from all sectors was 8, and assign no data when more than 2 sectors are empty. These parameters were kept constant all through the experiment for the purpose of maintaining consistence. One of the major factors that described the trend of Z value after estimation is the exponential component. In order words, different exponent power value results in a change in the output surface. Hence, different power values were used this research that is; $p\ = 2, 4, 6, 8, 10, 12, 14, 16, 18\ and\ 20$. Even exponent numbers "$p = 2, 4, \ldots, 20$" were used to avoid the complexity of data. Consequently, odd numbers (3, 5, 7, 13, 17, and 19) were not adopted in order to maintain uniforminity and it has no impact in the symmetrical shape of the reservoir. The volume of the reservoir was computed using trapezoidal and analyzed based on exponent employed.

3.1 Discussion of Cross-validation Output

The cross-validation report shows the results of the experiment conducted via inverse distance weighting depending on variate exponent number. Hence, the active data was 673, which obviously indicated that there are no excluded, deleted duplicates, retained duplicates, artificial, and superseded data, respectively. From table 1, it shows that the estimated nodes with spatial values are equal in $p = 2\ and\ p = 4$, but reduced by 3 in subsequent powers due to spread. Also, it will be observed that the coefficient of multiple determination (R^2) remained constant in all stages, which implies that there exists a homogeneity correlation between the measured and estimated data. However, there is a small additive decimal change in standard error which continue progressively by 0.001. Another component that changes is the coefficient of variation, but only at $p = 2, 4\ and\ 6$, others remained the same all through the processes. Conversely, the root mean square error varies according to exponent value and indicates that the results are reliable and that the interpolated sample are sufficiently spread. The univariate statistics of the Z component shows that the global variance increases progressively as the power factor was increased, indicating that exponent value influences the outcome of variance.

Table 1: Cross-validation results

IDW	R^2	Estimated Points	Standard Error	Coef of Variation	RMSE	Variance
$p = 2$	0.063	7400	0.035	0.012	1.046	9.312
$p = 4$	0.063	7400	0.042	0.015	0.138	12.930
$p = 6$	0.063	7397	0.045	0.016	0.007	14.772
$p = 8$	0.063	7397	0.046	0.017	0.032	15.887
$p = 10$	0.063	7397	0.047	0.017	0.051	16.657
$p = 12$	0.063	7397	0.048	0.017	0.063	17.217
$p = 14$	0.063	7397	0.049	0.017	0.074	17.636
$p = 16$	0.063	7397	0.049	0.017	0.083	17.954
$p = 18$	0.063	7397	0.049	0.017	0.091	18.199
$p = 20$	0.063	7397	0.050	0.017	0.097	18.388

4. RESULT AND DISCUSSION

The trend surface was assessed based on the varying exponential number and how it best fit or describe the data at the boundaries. Such assessment aided to know which exponent number is suitable for the determination of cubic content in a discrete object when IDW is applied to account for the sparse area of a dataset. To adequately compute the volumetric content a reservoir, it must have a definite shape and homogenous level in all sphere. Obviously, IDW spatial interpolation technique is adequate for estimating spatial data, because it maintains the data characteristic of maximum and minimum data limit, and even after interpolation the Z output is efficient and reliable. However, adhering to defined discrete boundaries is a major challenge at lower exponents power. This setback is described in figure 2 through figure 10 that is "figure $p = 2$ to figure $p = 18$" which indicated that the inferenced exceeded its defined boundaries thereby given false information about the surface beyond the maximum Z values. With this problem, calculating the cubic content based on the output will amount to determining the content of an open-ended object. An argument may be that the program should assign no data outside the convex hull of data, as shown in figure 12. The black area in figure 12 is the area where there are no estimated data as programmed before the experiment was conducted. This altered the shape and trend of the surface, which is not an exact replicate of the sample data. These figures (figure 2 to figure 10) described the inconsistency of exponent value to boundaries, but as the power value increases the external surface becomes levelled gradually making it suitable for the computation of volumetric content. At exponent $p = 20$, the external surface becomes almost even, and a closed discrete object, as illustrated in figure 11.

The dynamic surface trend beyond the boundaries varies continuously to an extent where the external surface equals the defined boundaries (figure 11). Figure 2 to figure 10 described the dynamic behavioural pattern of this spatial interpolation technique as it continues to change from grey to cyan and finally to complete blue representing equal level as shown in figure11. Usings the components considered for processing figure 12 will yield the desired volume of the discrete object when computed.

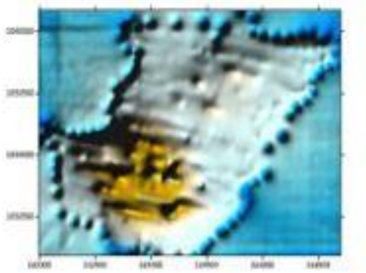

figure 2: $p = 2$

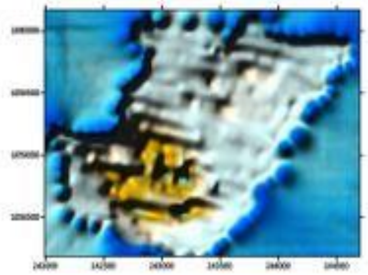

Figure 3: $p = 4$

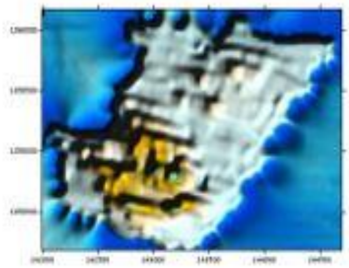

figure 4: $p = 6$

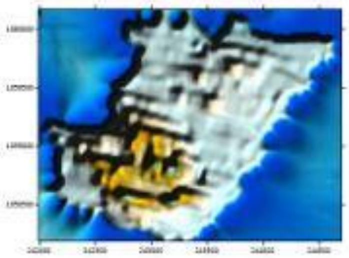

figure 5: $p = 8$

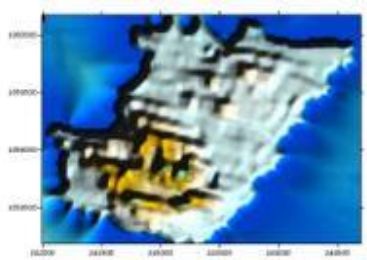

figure 6: $p = 10$

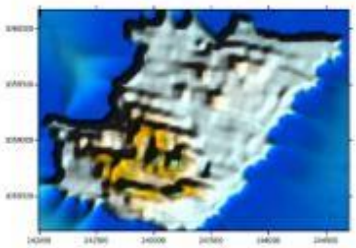

figure 7: $p = 12$

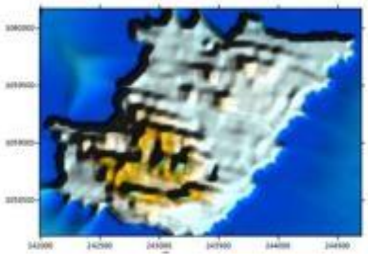

figure 8: $p = 14$

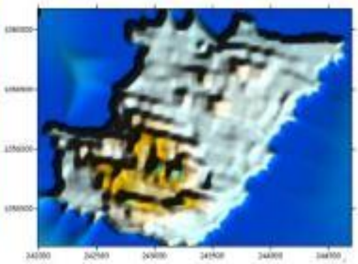

figure 9: $p = 16$

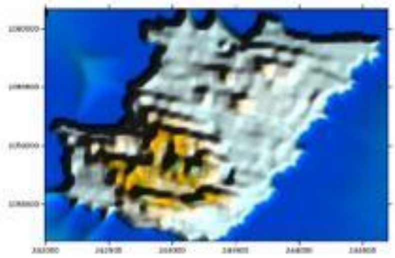

figure 10: $p = 18$

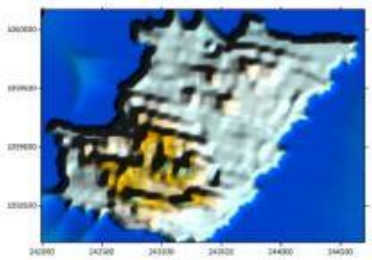

figure 11: $p = 20$

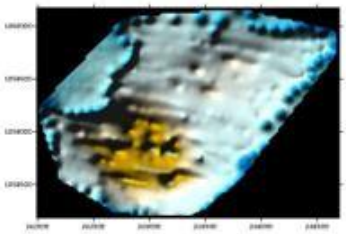

figure 11: $p = 2$ *Assign Nodata*

Figure 2-11 shows the relief digital elevation model and their behavoiral pattern based on different exponent number (source: research lab).

4.1 Volume computation on varying exponent

The volume of the irregular surface (Reservoir) was computed using trapezoidal rule based on different exponential number to assess the capacity of the container. Table 2 present the results of the enclosed surface of the discrete object; the outcome shows that the volumetric content increased progressively as the exponent power was enhanced, thus, describing the negative effect of lower exponent for interpolating discrete data. At lower power value the surface shape is altered at the edges making it looked like a flat surface. However, as the exponent number increases the shape at the boundaries started taking shape gradually and representing the actual enclosed container. This statement is supported by figure 2 to figure 11 above.

Table 2: Volume computation on varying exponent

Varying exponent value	Volume (m^3)	Percentage (%)
$p = 2$	87164733	9.537
$p = 4$	89100009	9.749
$p = 6$	90411448	9.892
$p = 8$	91285010	9.988
$p = 10$	91892165	10.055
$p = 12$	92326929	10.102
$p = 14$	92644192	10.137
$p = 16$	92878593	10.162
$p = 18$	93053254	10.182
$p = 20$	93184224	10.196
Total	**913940557**	**100.000**

Furthermore, the change in volume between $p = 2\ and\ p = 4$ which is 0.212% was greater compared to the difference between $p = 18\ and\ p = 20$ which equate to 0.014%, as the power number increases the change in volume between subsequent power becomes minimal. Therefore, suggesting that at a point the volume becomes equal irrespective of the exponent value.

5. CONCLUSION AND RECOMMENDATIONS

Inverse distance weighting of spatial interpolation technique has proven efficiency in handling open-ended data with adequate speed. However, its behavioural pattern to discrete data at the boundaries has not been investigated. Consequently, this research investigated the dynamic nature of this spatial estimation technique to discrete data (reservoir) based on varying the exponential number. The results demonstrated that IDW has the tendency of bull's-eye pattern at the boundaries as shown in figure 2, 3, and figure 4 that is "$p = 2, p = 4\ p = 6$"; on the other hand, as the exponent number was increased the menace gradually fadeaway and blended with the edges and then forming a better surface at the boundaries. Eventually, the constant level was homogenous all through the surface outwardly when $p = 20$. The volume computed increased as exponent number was evenly added from the starting point. Similarly, this method maintained the maximum and minimum data limit all through the experiment. Consequently, presenting an adequate digital elevation model of the discrete object (reservoir). Therefore, this research recommends a higher exponent number between the neighbourhood of 20 to 24 for interpolating discrete data when the cubic content is to be determined. Also, the shoreline should be adequately defined with equal level. Nevertheless, other methods of spatial interpolation can be used to inference bathymetric data. Also, this method (IDW) with varying exponent should be investigated by employing different software as the one used in this research is Surfer 17.

REFERENCES

Andreas, K., & Jukka, M. K. (2015). Spatio-temporal Visualization of Interpolated Particulate Matter (PM2.5) in Beijing. *Journal for Geographic Information Science, 6, 464-473* doi:10.1553/giscience2015s464.

Ajayi, O.G., Kuta, A.A., Osunde, J., & Ibrahim, P.O. (2018). Investigation of the robustness of different contour interpolation models for the generation of contour map and digital elevation models. *School of Environmental Technology Conference*, SETIC, 2018.

Ballarin, F., D'Amario, A., Perotto, S., & Rozza, G.(2017). A POD-Selective Inverse Distance Weighting method for fast parametrized shape morphing

Borga, M. & Vizzaccaro, A. (1997). On the interpolation of hydrologic variables: formal equivalence of multiquadratic surface fitting and kriging. *J Hydrol*, 195, 160–171

Diodato N, & Ceccarelli, M. (2005). Interpolation processes using multivariate geostatistics for mapping of climatological precipitation mean in the Sannio Mountains (southern Italy). *Earth Surface Process Land, 30,* 259–268

Deutsch, C.V. (2002). Geostatistical reservoir modeling. Oxford University Press, New York

Ferreira, I. O., Domingos, R. D. & Santos, G. R. (2015). Coleta, Processamento e Análise de dados batimétricos. *Novas edições acadê*

Franke, R. (1982). Scattered data interpolation: tests of some methods. *Math Comput* 38, 181-200

Goff, J.A., & Nordfjord, S. (2004). Interpolation of fluvial morphology using channel oriented coordinate transformation: a case study from the New Jersey shelf. *Mathematical Geology*, 36(6), 643-658.

Hansen, R.E., Saebo, T.O., Callow, H.J., Langli, B. & Hammerstad, E.O. (2007). Bathymetric Capabilities of the HISAS Interferometric Synthetic Aperture Sonar. *OCEANS2007*, *Vancouver*, *BC*,2007. doi:10.1109/OCEANS.2007.4449357

Hell, B., Broman, B., Jakobsson, L., Jakobsson, M., Magnusson, A., & Wiberg, P. (2012). The use of bathymetric data in society and science: a review from the Baltic Sea. *Ambio*, 41(2), 138–150. doi:10.1007/s13280-011-0192-y

Hilldale, R.C., & Raff, D., (2008). Assessing the ability of airborne LiDAR to map river bathymetry. *Earth Surface Processes and Landforms*, 33 (5), 773–783.

https://www.iho.int/srv1/index.php?option=com_content&view=article&id=299&Itemid=289&lang=en

Ingham, A.E. (1984). Hydrography for the Surveyor and Engineer. New York: *John Wiley & Sons*. pp. 1. ISBN 0-471-80535-1

Journel, A.G. & Huijbregts, Ch. J. (1978). Mining Geostatistics. London & New York (Academic Press), 1978. x 600 pp., 267 figs. Price £32·00. Mineralogical Magazine, 43(328), 563-564. doi:10.1180/minmag.1979.043.328.34

Lampe, D.C., & Morlock, S.E. (2007). Collection of bathymetric data along two reaches of the Lost River within Bluespring Cavern near Bedford, Lawrence County, Indiana. US G.

S. *Scientific Investigations Report* 2008-5023, 142 p.<http://pubs.water.usgs.gov/sir>2008-5023.
Landim, P. M. B., Sturaro, J. R., & Monteiro, R. C. (2000). Krigagem ordinária para situações com tendência regionalizada. *Revista Laboratório Geomat*, pp.06-12
Lark, R. M. (2009). Kriging a soil variable with a simple nonstationary variance model. *Journal of Agricultural, Biological and Environmental Statistics*, 14(3), 301-321
Marcelo, C., Joaquim, L., Igor, O., Joao, L., and Jose, S. (2015). Assessment of Spatial Interpolation Methods to Map Bathymetry of an Amazonian Hydroelectric reservoir to Aid in decisition marking for water Management. *ISPRS International Journal of Geo-Informatics, 4, 220-235.* doi: 10.3390/ijgi4010220
Marian, M., Dongsu, K., & Venkatesh, M. (2012). Gravel Bed: Processes, Tools, Environmental; Modern Digital Instruments and Morphologic Characterization of River Channels. pp315-321, *John Wiley & Sons Ltd*, UK.
Meng, Q. Liu, Z. and Borders, B. E. (2013). Assessment of regression kriging for Spatial interpolation—Comparisons of seven GIS interpolation methods. *Cartography and geographic information science*, 40, 28–39.
Merwade, V. M., Maidment, D. R., & Goff, J. A. (2006). Anisotropic considerations while interpolating river channel bathymetry. *Journal of Hydrology*, 331, 731–741.
Nalder, I.A. & Wein, R.W. (1998). Spatial interpolation of climatic normals: test of a new method in the canadian boreal forest. *Agric Forest Meteorol*, 92, 211–225
Noel, C. & Andrew, Z. (2016). Multivariate Spatial Covariance Models: A Conditional Approach. Retrieved on 12/16/19 from https://arxiv.org/pdf/1504.01865.pdf
Ojigi, M. L., Mohammed, S. O., & Jeb, D. N. (2010). Pre-Dredging and Navigational Potential Analysis of the Niger-Benue Confluence Area, Lokoja, Nigeria Using Remote Sensing and GIS. *8th AARSE International Conference [AARSE2010]*, UNECA Hqtrs, Addis Ababa Ethiopia
Olena, B. & Clayton, V. D. (2008). Statistical approach to inverse distance interpolation. *Stochastic Environmental Research and Risk Assessment, 23(5), 543-553.* doi 10.1007/s00477-008-0226-6
Petersen, C.T., Trautner, A., Hansen, S. (2008). Spatio-temporal variation of anisotropyof saturated hydraulic conductivity in a tilled sandy loam soil. *Soil and Tillage Research* 100 (1–2), 108–113.
Shepard, Donald (1968). "A two-dimensional interpolation function for irregularly-spaced data". Proceedings of the 1968 ACM National Conference. pp. 517–524. doi:10.1145/800186.810616
Silveira, T. A., Portugal, J. L., Sá, L. A. C. M., & Vital, S. R. O. (2014). Análise estatística espacial aplicada a construção de superfícies batimétricas. *Geociências*, 33(4), pp.596-615
Stefan, W., Bernat, M., Knut, H., Martin, V., Tim, T., Simon, L., & Dick, S. (2017). The BASE-platform project: Deriving the bathymetry from combined satellite data. *Hydrographische nachrichten-Fachzeitschrift für Hydrographie und Geoinformation,* HN (101), pp20-23.
Vermeyen, T. B. (2006). Using an ADCP, depth sounder, and GPS for bathymetric surveys. In: *Proceedings of the ASCE World and Environmental Resources Congress*, Omaha, NE

White, L., & Hodges, B.R., (2005). Filtering the Signature of submerged large woodydebris from bathymetry data. *Journal of Hydrology*, 309 (1–4), 53–65.
Yongwan, C. & Daniel, A.G. (2013). Spatial Statistics & Geostatistics: Methods for spatial interpolation in two dimensions. p27. SAGE Publications Ltd, London.

BIOGRAPHICAL NOTES

Pius Onoja Ibrahim is a PhD research student at the Department of Hydrography and Geodesy, HafenCity University Hamburg, Germany. He is an assistant lecturer with the Department of Surveying and Geoinformatics, Federal University of Technology Minna, Niger state, Nigerian. His interest in hydrography as propel him to conduct several researches on Dams and rivers in Nigeria. He is looking forward in contributing is own quata to the body of Hydrographers in a global context.

Prof. Dr.-Ing. Harald Sternberg is professor for Hydrography and Geodesy at the HafenCity University Hamburg since 2018, before that he was professor for Engineering Geodesy and Geodetic Metrology since 2001. Beside his research activities in the field of Hydrography, Indoor Navigation and data-driven Analysis, he is the Vice President for Teaching and Studies at the HCU.

CONTACTS

Pius Onoja Ibrahim,
Hydrography and Geodesy
HafenCity University
Überseeallee 16, 20457
Hamburg,
GERMANY

Department of Surveying and Geoinformatics
Federal University of Technology Minna
Niger State
NIGERIA
Email pius.ibrahim@hcu-hamburg.de or pius.onoja@futminna.edu.ng

Prof. Dr.-Ing. Harald Sternberg Harald
Hydrography and Geodesy
HafenCity University
Überseeallee 16,
20457 Hamburg,
GERMANY
Email: harald.sternberg@hcu-hamburg.de Web site: https://www.hcu-hamburg.de/